INVITED PAPER *Special Section on Recent Progress in Antennas and Propagation Researches*

MIMO Propagation Channel Modeling*

Yoshio KARASAWA[†a)], ***Member***

SUMMARY This paper provides an overview of research in channel modeling for multiple-input multiple-output (MIMO) data transmission focusing on a radio wave propagation. A MIMO channel is expressed as an equivalent circuit with a limited number of eigenpaths according to the singular-value decomposition (SVD). Each eigenpath amplitude depends on the propagation structure not only of the path direction profiles for both transmission and reception points but also of intermediate regions. Inherent in adaptive control is the problem of instability as a hidden difficulty. In this paper these issues are addressed and research topics on MIMO from a radio wave propagation viewpoint are identified.

key words: *MIMO, singular-value decomposition, multipath fading, eigenvalue distribution, spatial correlation, diversity, maximum ratio combining*

1. Introduction

Research on information transmission using a multiple-input multiple-output (MIMO) configuration involving the use of an array antenna for both transmission and reception has gained momentum in recent years. This interest has been spurred by the practical implementation of arrays of terminals, as seen in wireless local area networks (LANs), providing the highly efficient transmission of information.

In terms of its scientific underpinnings, research on MIMO can be broadly divided into (i) research on array antennas and adaptive signal processing [1]–[8] for the implementation of antenna configurations and control methods, (ii) research on information theory and coding schemes (space-time coding) [9]–[12] for the implementation of efficient data transmission, and (iii) research on radio wave propagation [13]–[18] for the modeling of MIMO channel.

From the viewpoint of radio wave propagation, MIMO is closely related to the space-domain signal processing techniques, such as the space diversity and adaptive array techniques. Specifically, the arrival angle spreading of multipath waves and the associated spatial correlation characteristics have a significant impact on the information transmission capacity of MIMO. The modeling of a MIMO channel, if attempted rigorously, requires sophisticated knowledge of numerical statistics [19]–[22]. Even with the use of such tools, however, only a very limited number of models, such as i.i.d. (independent identically distributed) channels, have been solved mathematically. Against the background of these research efforts, this paper addresses radio wave propagation as the key to the data transmission capacity of MIMO channels, and provides a general review of research on propagation channel modeling. After discussing the basic principles necessary to understand the mechanism of MIMO data transmission, the latest research effort, such as the modeling of channels that considers space correlation characteristics [23], a topic which we have pursued is presented.

This paper is organized as follows: First, focusing on the angular spread of multipath waves, the radio wave propagation environment for mobile communications is discussed in Sect. 2. A propagation channel representation of MIMO channels is then presented with respect to narrowband and broadband signals in Sect. 3, and the critical role of the eigenvalue in the correlation matrices is discussed in the context of propagation channel representation. Based on the results presented in Sect. 3, the statistical characteristics of MIMO channels are clarified in Sect. 4 by addressing cases in which the correlation between branches can be ignored and those in which it must be taken into consideration. The problem of the instability of weight control is also considered in Sect. 5 as a unique feature of MIMO, and important research topics for MIMO are finally identified from a radio wave propagation viewpoint in Sect. 6.

2. Radio Wave Propagation Environment for Mobile Communications

The radio wave propagation environment for mobile communications including portable terminals for use in wireless LANs is a multipath environment characterized by reflection, scattering, diffraction, and blocking. Focusing on the angular spread of the multipath environment, the propagation environment is classified, as shown in Fig. 1, into two types: Model 1 is a propagation path model in which both the transmitting and receiving stations exist in the same scattering area, and Model 2 is a propagation path model in which one station exists in a locally distributed scattering area and the other station is in a position with a clear view of the scattering area. Representative examples of Model 1 may be an indoor propagation environment (wireless LAN, etc.) and a propagation channel for mobile communications with low base-station-antenna-height systems. Typical cases

Manuscript received December 10, 2004.
Manuscript revised January 27, 2005.

[†]The author is with the Department of Electronic Engineering, The University of Electro-Communications, Chofu-shi, 182-8585 Japan.

*This article was originally published in the IEICE Transactions on Communications (Japanese Edition), vol.J86-B, no.9, pp.1706–1720, Sept. 2003.

a) E-mail: karasawa@ee.uec.ac.jp

DOI: 10.1093/ietcom/e88–b.5.1829

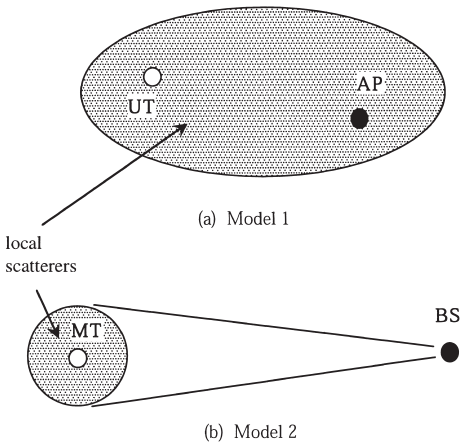

Fig. 1 Classification of mobile propagation channels. (UT: user terminal, AP: access point, MT: mobile terminal, BS: base station)

of Model 2, on the other hand, may be propagation channels involving mobile communications with high base-station-antenna-height systems.

Both access points (APs) and user terminals (UTs) in Model 1, and mobile stations (MSs) in Model 2, are suitable for modeling if it is assumed that either the probability of the direction of paths is uniformly distributed in the horizontal plane or the angular spread of the paths is sufficiently large. If the angles of arrival are uniformly distributed, the spatial correlation ρ_a can be expressed as

$$\rho_a(\Delta x)\left(\equiv \frac{\langle a^*(x)a(x+\Delta x)\rangle}{\langle a^*(x)a(x)\rangle}\right) = J_0(k\Delta x) \quad \text{(for AP, UT, MS),} \quad (1)$$

where Δx denotes the distance between antennas, a is a complex amplitude representing the channel response, J_0 is a zeroth-order Bessel function, k is the wavenumber of the radio waves, and $\langle\ \rangle$ denotes the ensemble average. In Model 2, under the assumption that the path-direction distributes normally over a relatively narrow range (namely, the standard deviation of angular spread, σ_θ, is much smaller than unity) centered around the direction of the mobile terminal (angle from the frontal direction of the antenna: θ_0), the spatial correlation can be expressed as [24]

$$\rho_a(\Delta x) = \exp\left(jk\Delta x \sin\theta_0 - \frac{k^2\Delta x^2 \sin^2\theta_0\sigma_\theta^2}{2}\right) \quad \text{(for BS).} \quad (2)$$

Figure 2 shows the calculated values of the space correlation $\rho(\equiv|\rho_a|)$ represented by Eqs. (1) and (2) in Rayleigh fading environment. Note that $|\rho_a|^2$ with a different definition is sometimes used in the literature (e.g., [24], [25]) as a correlation coefficient. From the figure, it is evident that in an environment (AP, UT, or MS) in which the spatial correlation is expressed by Eq. (1), signal variations can be treated as independent if the antennas are located at distances greater than half the wavelength. At the base station

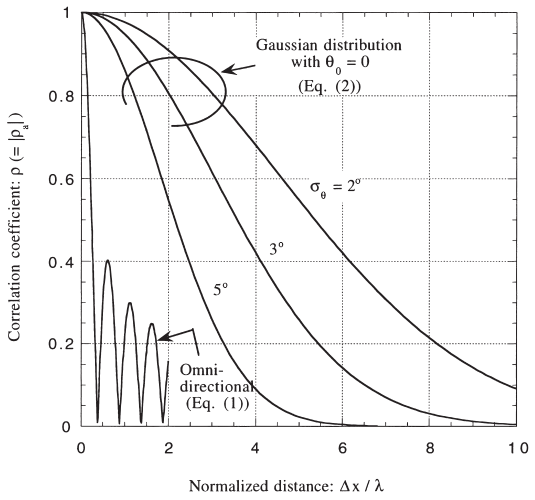

Fig. 2 Correlation characteristics in Rayleigh fading environment.

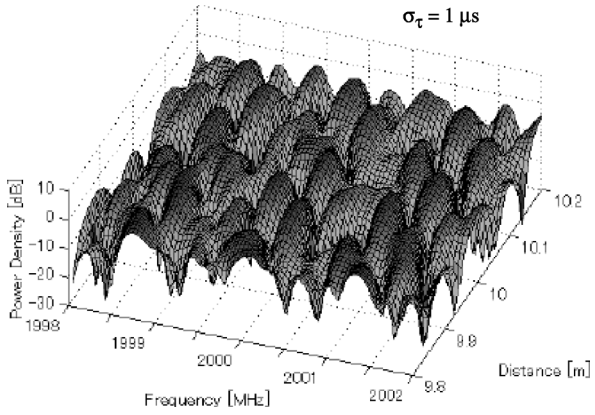

Fig. 3 Transfer function of multipath channel.

(BS) represented by Eq. (2), on the other hand, there exists a considerable spatial correlation depending on the angular spread of paths. For example, if $\sigma_\theta = 3°$, the correlation coefficient will be approximately 0.8 for a distance of approximately 2 wavelengths, and the correlation between antennas may therefore be taken into account.

Figure 3 shows the frequency characteristics (transfer function) of a multipath channel simulated assuming typical mobile communications in an urban environment (Model 2), and illustrates the manner in which the frequency characteristics change as a function of spatial position [26]. Several dips (drops in transmission characteristics) are visible in the 4 MHz band centered around 2 GHz. These dips, caused by the spread of delay in multipath waves, produce distortion of the transmission waveform with respect to the broadband signals. As such characteristics change drastically with only a slight change in position (of the order of 10 cm), the characteristics can fluctuate rapidly with time in high-speed moving bodies such as vehicles. The adaptive signal processing scheme for mobile communications can be regarded as a technique that realizes reliable communications by overcoming the problem of irregularities in the frequency

and time regions, as illustrated in Fig. 3.

3. Representation of MIMO Propagation Channels

For an intuitive understanding of spatial signal processing, we first consider signal transmission in free space using a 4×4-element MIMO, (Fig. 4). If the distance between antenna elements is sufficiently large and the distance of transmission is relatively short (Fig. 4(a)), several methods of data transmission are possible. For example, successive signals $s_1 s_2 s_3 s_4 s_5 s_6 s_7 s_8 \ldots$ can be divided among antennas 1-4 and transmitted in groups of $s_1 s_5 \ldots$, $s_2 s_6 \ldots$, $s_3 s_7 \ldots$, and $s_4 s_8 \ldots$, respectively. Although the received signals are subject to some cross-interference, this problem can be solved through signal processing at the receiving site. Carrying this analysis a step further, if the distance between arrays is made sufficiently large (Fig. 4(b)), information transmitted by dividing between antenna elements cannot be separated spatially at the receiving site, and the transmission mode depicted in Fig. 4(a) no longer works. In this case, the only viable option is to orientate each antenna beam with respect to each opposite station. In terms of the propagation channel model that is discussed later, the former approach represents the situation where approximately four eigenpaths of roughly the same amplitude exist in the channel, whereas the latter approach represents the situation where the paths have collapsed into one. The former case permits various modifications of the data transmission scheme and is potentially useful for high-speed data transmission. Since in multipath environments, a number of such eigenpaths exist even when the distance between arrays is large, MIMO data transmission is characterized by the effective utilization of path multiplicity.

Figure 5 shows the basic configuration of the data transmission scheme in MIMO. To achieve data transmission by exploiting environmental characteristics, which involves the use of multiple antennas, the transmitter performs coding in space and time regions, as shown in Fig. 4(a), and the receiver performs the decoding. There are two categories for data transmission whether the transmitting site has the channel state information (CSI) or not. Case 1 in the figure is that in which the transmitting site does not have CSI, while Case 2 is information is shared between the transmitter and receiver. The two cases involve different methods of data transmission. In the following section, the representation of the propagation channel is discussed.

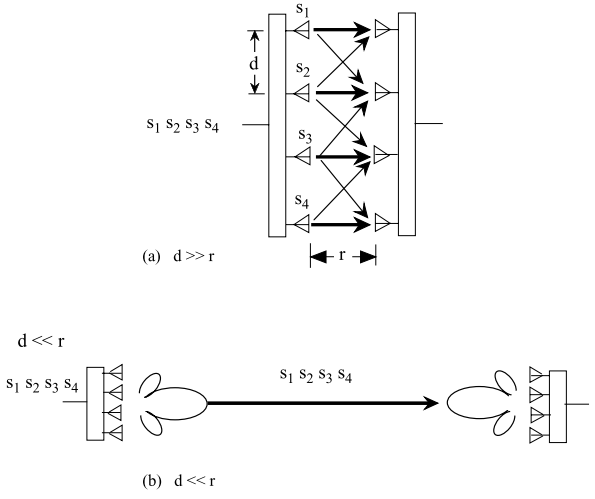

Fig. 4 Data transmission scheme for MIMO channel in free space environment.

3.1 Propagation Channel Representation for Narrow-Band Signals

Consider a channel with M transmission antennas and N reception antennas. The channel response (CSI) between the arrays can be expressed by the following matrices:

$$A = [\, \boldsymbol{a}_1 \; \boldsymbol{a}_2 \; \ldots \; \boldsymbol{a}_m \; \ldots \; \boldsymbol{a}_M \,] \tag{3a}$$

$$\boldsymbol{a}_m = [\, a_{1m} \, a_{2m} \; \ldots \; a_{nm} \; \ldots \; a_{Nm} \,]^T, \tag{3b}$$

where superscript T denotes transposition.

The channel response matrix A can be expressed as follows in a singular-value decomposition (SVD) (e.g., [13]).

$$A = E_r D E_t^H = \sum_{i=1}^{M_0} \sqrt{\lambda_i}\, \boldsymbol{e}_{r,i} \boldsymbol{e}_{t,i}^H, \tag{4}$$

where

$$D \equiv \mathrm{diag}\left[\sqrt{\lambda_1} \; \sqrt{\lambda_2} \; \ldots \; \sqrt{\lambda_{M_0}} \right] \tag{5}$$

$$E_t \equiv [\, \boldsymbol{e}_{t,1} \; \boldsymbol{e}_{t,2} \; \ldots \; \boldsymbol{e}_{t,M_0} \,] \tag{6}$$

$$E_r \equiv [\, \boldsymbol{e}_{r,1} \; \boldsymbol{e}_{r,2} \; \ldots \; \boldsymbol{e}_{r,M_0} \,] \tag{7}$$

$$M_0 \equiv \min(M, N). \tag{8}$$

Superscript H denotes a complex conjugate transposition, λ_i is the ith eigenvalue of the correlation matrix AA^H (or $A^H A$) for $i = 1, 2, \ldots, M_0$ (in descending order), $\boldsymbol{e}_{t,i}$ is the eigenvector belonging to the eigenvalue λ_i of matrix $A^H A$, and $\boldsymbol{e}_{r,i}$ is the eigenvector belonging to the eigenvalue λ_i of matrix AA^H.

When decomposed in this manner, the propagation

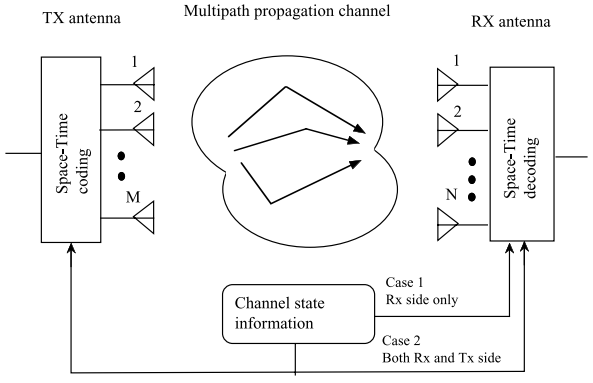

Fig. 5 Data transmission scheme in MIMO configuration.

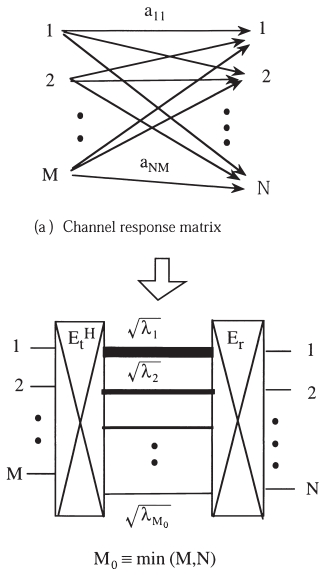

Fig. 6 Equivalent circuit of MIMO channel based on SVD.

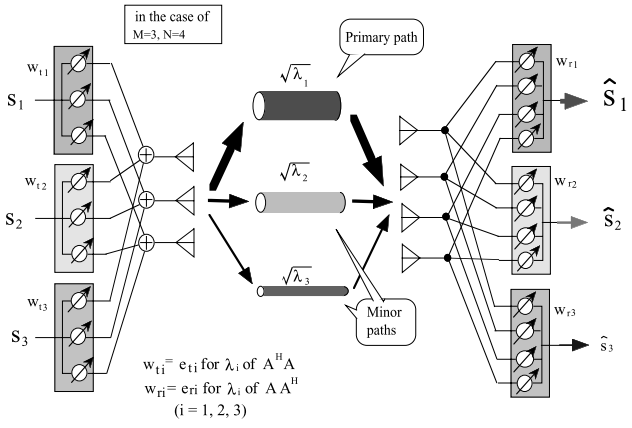

Fig. 7 Parallel data transmission scheme through each eigenpath.

path for a MIMO channel can be represented as in Fig. 6, where (a) shows the equivalent circuit representing Eq. (3), and (b) is the equivalent circuit represented in SVD. It is clear that the MIMO channel comprises a maximum of M_0 (the smaller of M and N) independent transmission paths. In this context, the term "maximum" refers to the maximum possible number of actual paths. If there are multiple paths for which the eigenvalue is 0, the number of paths will be reduced even further. Such virtual paths are referred to as eigenpaths. The amplitude gain for each unique path is $\sqrt{\lambda_i}$, and it varies according to its eigenvalue. Thus, the MIMO channel possesses the capacity to transmit M_0 independent streams of signals without cross-talk. Figure 7 shows the specific configuration of an eigenmode transmission scheme.

Next, consider transmission in which data transmitted through only the largest eigenpath is received with the maximum signal-to-noise ratio (SNR) with transmission/reception weight control, that is, maximal ratio combining (MRC) transmission. Here, the transmission antenna weight vector is $\boldsymbol{w}_t(\equiv [w_{t,1}, w_{t,2}, \ldots, w_{t,M}]^T)$, the receiver antenna weight vector is $\boldsymbol{w}_r(\equiv [w_{r,1}, w_{r,2}, \ldots, w_{r,N}]^T)$, which are normalized by $\boldsymbol{w}_r^H \boldsymbol{w}_r = 1$ and $\boldsymbol{w}_t^H \boldsymbol{w}_t = 1$, the noise component vector is $\boldsymbol{n}(t)(\equiv [n_1(t), n_2(t), \ldots, n_N(t)]^T)$, and the transmitting signal is s. The reception signal and its average power are respectively given by

$$\hat{s}(t) = \boldsymbol{w}_r^H (A\boldsymbol{w}_t s(t) + \boldsymbol{n}(t)) \tag{9}$$

$$\langle |\hat{s}(t)|^2 \rangle = \lambda \langle |s(t)|^2 \rangle + \langle |n_1(t)|^2 \rangle \tag{10}$$

$$\lambda = \boldsymbol{w}_r^H A \boldsymbol{w}_t \boldsymbol{w}_t^H A^H \boldsymbol{w}_r = \boldsymbol{w}_t^H A^H \boldsymbol{w}_r \boldsymbol{w}_r^H A \boldsymbol{w}_t, \tag{11}$$

where n_1 is the noise component of antenna 1. Because the average power of noise for the various branches is equal, the quantity n_1 is used as the representative component.

As λ in Eq. (11) is a gain factor of the SNR, setting $\boldsymbol{w}_t$ and $\boldsymbol{w}_r$ such that λ becomes maximum will allow for transmission with the maximum SNR using the weight of the set ($\boldsymbol{w}_t$ and $\boldsymbol{w}_r$). The set can be determined using Lagrange's multiplier method, as

$$\varphi(\boldsymbol{w}_t, \boldsymbol{w}_r, \lambda_t, \lambda_r) = \lambda - \lambda_t(\boldsymbol{w}_t^H \boldsymbol{w}_t - 1) - \lambda_r(\boldsymbol{w}_r^H \boldsymbol{w}_r - 1) \tag{12}$$

$$\frac{\partial \varphi}{\partial \boldsymbol{w}_r} = 2A\boldsymbol{w}_t \boldsymbol{w}_t^H A^H \boldsymbol{w}_r - 2\lambda_r \boldsymbol{w}_r = 0 \tag{13}$$

$$\frac{\partial \varphi}{\partial \boldsymbol{w}_t} = 2A^H \boldsymbol{w}_r \boldsymbol{w}_r^H A \boldsymbol{w}_t - 2\lambda_t \boldsymbol{w}_t = 0. \tag{14}$$

The problem then reduces to the eigenvalue problem given by the following set of simultaneous equations:

$$\left[A\boldsymbol{w}_t \boldsymbol{w}_t^H A^H\right] \boldsymbol{w}_r = \lambda_r \boldsymbol{w}_r \tag{15}$$

$$\left[A^H \boldsymbol{w}_r \boldsymbol{w}_r^H A\right] \boldsymbol{w}_t = \lambda_t \boldsymbol{w}_t. \tag{16}$$

Equations (15) and (16) can be transformed into the form of Eq. (11) as follows.

$$\boldsymbol{w}_r^H \left[A\boldsymbol{w}_t \boldsymbol{w}_t^H A^H\right] \boldsymbol{w}_r = \boldsymbol{w}_r^H \lambda_r \boldsymbol{w}_r = \lambda_r \tag{17}$$

$$\boldsymbol{w}_t^H \left[A^H \boldsymbol{w}_r \boldsymbol{w}_r^H A\right] \boldsymbol{w}_t = \boldsymbol{w}_t^H \lambda_t \boldsymbol{w}_t = \lambda_t. \tag{18}$$

where both λ_r and λ_t are possible values of λ, as physical quantities corresponding to the reception power or SNR.

The meaning of Eq. (15) can be interpreted as follows. Although λ_r is the eigenvalue of the matrix $[A\boldsymbol{w}_t \boldsymbol{w}_t^H A^H]$, as we are seeking the maximum value of λ_r, the maximum eigenvalue $\lambda_{r,\max}$ is the maximum value of the desired reception power. The weight that produces the maximum value is the eigenvector $\boldsymbol{e}_{r,\max}$ of the maximum eigenvalue. However, as this equation contains the quantity $\boldsymbol{w}_t$, it cannot be solved directly. Similarly, in Eq. (16), the maximum eigenvalue $\lambda_{t,\max}$ is the maximum value of the desired reception power, and the weight that produces it is an eigenvector $\boldsymbol{e}_{t,\max}$ of the desired reception power.

Note that in Eq. (15), the matrix $[A\boldsymbol{w}_t \boldsymbol{w}_t^H A^H]$ is comprised of the product of a vector $A\boldsymbol{w}_t$ and its Hermitian transposition. Therefore, its non-zero eigenvalues $\lambda_{r,\max}$ form a

matrix of rank 1. The eigenvector of that matrix will be a vector that is obtained by normalizing the vector $A\boldsymbol{w}_t$. Similarly, in Eq. (16), in the matrix $[A^H \boldsymbol{w}_r \boldsymbol{w}_r^H A]$, the nonzero eigenvalues $\lambda_{t,\max}$ form a unique matrix of rank 1. Therefore, the eigenvector with eigenvalues $\lambda_{r,\max}$ and $\lambda_{t,\max}$ can be represented by

$$\boldsymbol{e}_{r,\max} = \boldsymbol{w}_r = \frac{1}{\sqrt{\lambda_{r,\max}}} A\boldsymbol{w}_t \tag{19}$$

$$\boldsymbol{e}_{t,\max} = \boldsymbol{w}_t = \frac{1}{\sqrt{\lambda_{t,\max}}} A^H \boldsymbol{w}_r. \tag{20}$$

From these two equations, we obtain

$$A^H A \boldsymbol{w}_t = \sqrt{\lambda_{r,\max}\lambda_{t,\max}}\, \boldsymbol{w}_t \tag{21}$$

$$AA^H \boldsymbol{w}_r = \sqrt{\lambda_{r,\max}\lambda_{t,\max}}\, \boldsymbol{w}_r. \tag{22}$$

This reduces the weight to be determined to the familiar eigenvalue problem. Furthermore, the following equation can be obtained from Eqs. (11), (17), and (18):

$$\lambda_{r,\max} = \lambda_{t,\max} \equiv \lambda_{\max}. \tag{23}$$

Thus, the maximum value will be the maximum eigenvalue of the Hermitian matrix $A^H A$ (or AA^H), and the weights for the transmitter and receiver will be

$$\boldsymbol{w}_t = \boldsymbol{e}_{t,1}, \quad \boldsymbol{w}_r = \boldsymbol{e}_{r,1}. \tag{24}$$

This corresponds to an eigenmode transmission using the largest eigenpath shown in Fig. 7, and the transmission in which all power is assigned solely to the eigenpath will realize MRC transmission. This transmission method, in which the transmission and reception processes are controlled optimally with respect to the antenna pattern, is also referred to as eigen-beam-forming transmission.

The MRC transmission method represents transmission via the primary path of channels. In contrast, multistream transmission [8] can be interpreted as transmission using the second or lower eigenvalue path, that is, minor paths. Figure 8 shows a simple example of the latter approach, where considerable benefits are gained through the use of both the primary path and minor paths.

The figure illustrates the case where the primary and minor paths are of the same width, that is, where two eigenpaths with equal eigenvalues are available. Figure 8(a) shows the case where all power is assigned to one of the paths and 4 bits per symbol are transmitted by 16-QAM. By contrast, Fig. 8(b) shows the case where information is transmitted via two paths by halving the power assigned to each path by QPSK. There is a fourfold difference between QPSK and 16-QAM in terms of the carrier wave to noise ratio (CNR), at which the error rates are the same for the two paths. Thus, even when the transmission power is divided equally, the method described in Fig. 8(b) can achieve a lower error rate. If the error rates are to be equalized, a modulation method (e.g., 8-QAM) that permits 3-bits-per-symbol transmission should be adequate if two paths are

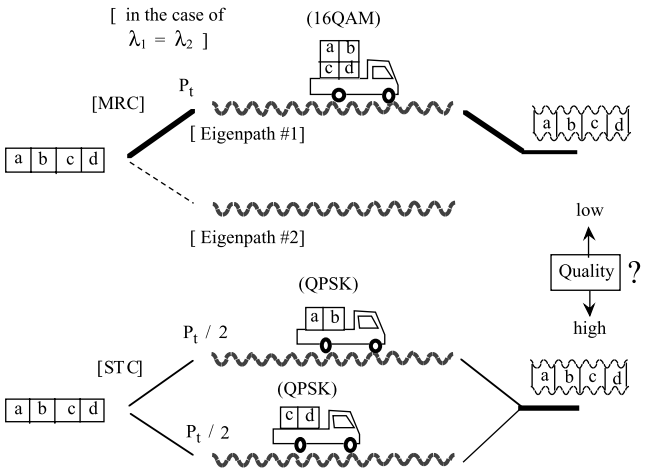

Fig. 8 Is it possible to increase channel quality when utilizing all of the eigenpaths?

used. Thus, the figure illustrates that in transmission paths with high SNR, the use of other eigenpaths (minor paths) is more efficient than transmitting information solely over the largest eigenpath (primary path).

However, what happens in cases with low SNR? For example, consider substituting QPSK, a 2-bit transmission scheme, for the 16-QAM portion in Fig. 8(a). To achieved the same result as in Fig. 8(b), BPSK is employed as the modulation method. However, in this case, given the relationship between the signal-to-noise ratio (SNR) and the bit error rate (BER), it is clear that the use of BPSK yields little benefit. Thus, it is clear that the effect of MIMO is significantly dependent not only on the number of antennas employed, but also on the SNR of the propagation channel.

In cases where the transmitter does not possess information on the transmission path (Case 1 in Fig. 5), the key to achieve adequate performance in the worst-case scenario will be to use a transmission method that minimizes transmission deterioration. If the same signals (coherent signals) are transmitted from the transmitter using a multiple-element antenna, null points occur in certain directions, as seen in an antenna pattern for an array antenna. The worst case is the condition in which a path exists in such a null-point direction. Such a transmission method does not conform to this paradigm.

For cases involving the use of a two-element antenna on the transmitter side, Alamouti devised a method in which, for information s_1 and s_2 to be transmitted, one antenna transmits s_1 and $-s_2^*$, and the other antenna transmits s_2 and s_1^*, and the receiver performs block decoding using channel state information (CSI) as prior knowledge. However, due to the fact that the transmitter does not posses knowledge of the channel, the reception capacity suffers a reduction in SNR equivalent to 3 dB, compared with the MRC used in Case 2 [9]. Transmission in which signals are rearranged in both the space and time domains in this manner is referred to as space-time block coding (STBC) transmission. Based on the transmission method proposed

by Alamouti, there has been active research interest in expanding the application of the method. Although further treatment of the STBC technique is beyond the scope of this paper, interested readers can obtain more information in Refs. [9]–[12].

3.2 Wideband Signal

In the preceding section, an equivalent circuit representation was given for narrow-band transmission paths in which the MIMO transmission path does not have frequency characteristics. In this section, the situation where frequency-selective characteristics within a band become irregular due to the spread of delay in multipath waves, that is, a MIMO transmission path representation with respect to frequency-selective fading, is considered.

Suppose that h_{nm} denotes the impulse response of a transmission path (with, m, transmission antenna and, n, reception antenna, presented simply as h in the present discussion) between arbitrary sets of antennas, and consider an approximate representation of impulse response for the situation in which the spreading of multipath delay is greater than the symbolic period T_s of the modulation signal. The channel impulse response is assumed to include the characteristics of a band-limited filter, and the receiver is assumed to perform several sampling operations per symbol. The description of the model will therefore depend on system parameters.

If the propagation paths represent a time-invariant system, impulse response h and impulse response $\bar{h}$ of a band-limited channel are respectively given as

$$h(\tau) = \sum_i a_i \delta(\tau - \tau_i) \tag{25}$$

$$\bar{h}(\tau) = \sum_i a_i g(\tau - \tau_i), \tag{26}$$

where a_i and τ_i denote the complex amplitude and the amount of delay of the elementary wave i, δ is the delta function, and g is the impulse response of the band-limiting filter. The filter used for band-limiting is either a Nyquist or Gaussian filter. The bandwidth B of the filter is often designed such that BT_s with respect to the symbol period T_s is approximately 1.

The signal to be transmitted, assuming that it is an impulse that is generated in each symbolic period T_s, is given by

$$s(t) = \sum_{k=-\infty}^{\infty} d(k)\delta(\tau - kT_s), \tag{27}$$

where $d(k)$ is the time series of transmitted data, which is treated as an infinitely continuing series.

The reception waveform (exclusive of noise components) for the modulation signals subject to band restrictions is given by

$$\begin{aligned} s_R(t) &= s(t) \otimes \bar{h}(t) \\ &= \sum_{k=-\infty}^{\infty} \left\{ d(k) \sum_i a_i g(t - kT_s - \tau_i) \right\}, \end{aligned} \tag{28}$$

where $\otimes$ denotes a convolution. If this signal is sampled at time $t = kT_s$, the resulting output will be

$$\begin{aligned} s_R(kT_s) = \cdots &+ d(k-1)\bar{h}(T_s) + d(k)\bar{h}(0) \\ &+ d(k+1)\bar{h}(-T_s) + \cdots . \end{aligned} \tag{29}$$

In a system where sampling is performed with symbol period (T_s) timing, the impulse response of the transmission path is equivalent to the following equation with respect to impulses at intervals of T_s:

$$\bar{h}_e(\tau) = \sum_{k'=-\infty}^{\infty} \bar{h}(k'T_s)\delta(\tau - k'T_s). \tag{30}$$

In one-sample-per-symbol operations, such as the equalization of multipath waveform distortion, the performance evaluation of adaptive arrays, or operation analyses based on simulations, the number of multipath waves that can be incorporated is insufficient. To circumvent this problem, two and four samples per symbol period are often employed.

The equivalent impulse response for J samples per symbol can be expressed as

$$\begin{aligned} \bar{h}_e(\tau) = \sum_{k'=-\infty}^{\infty} \sum_{j=1}^{J} &\bar{h}\left\{\left(k' + \frac{j-1}{J}\right)T_s\right\} \\ &\cdot \delta\left\{\tau - \left(k' + \frac{j-1}{J}\right)T_s\right\}. \end{aligned} \tag{31}$$

Thus, in situations where the spread of the impulse response of a propagation channel is greater than the symbol period T_s of the modulation signal, the impulse response can be converted equivalently to an impulse response that is rendered discrete in T_s/J. In this case, the reception signal can be determined as

$$s_R\left(\frac{\ell T_s}{J}\right) = \sum_{k=-\infty}^{\infty} \left[d(k)\bar{h}\left\{\left(-k + \frac{\ell}{J}\right)T_s\right\}\right], \tag{32}$$

where ℓ is an integer that represents the temporal order of sampling, and the range of k that provides a substantial contribution is the range equivalent to the spread of the delay centered around ℓ/J.

In the case of a MIMO channel, the equivalent impulse response matrix $\bar{H}_e(\tau)$ can be expressed by

$$\begin{aligned} \bar{H}_e(\tau) = \sum_{k''=-\infty}^{\infty} &\begin{bmatrix} \bar{h}_{11}\left(\frac{k''}{J}T_s\right) & \ddots & \\ \ddots & \bar{h}_{nm}\left(\frac{k''}{J}T_s\right) & \ddots \\ & \ddots & \bar{h}_{NM}\left(\frac{k''}{J}T_s\right), \end{bmatrix} \\ &\cdot \delta\left(\tau - \frac{k''T_s}{J}\right), \end{aligned} \tag{33}$$

where $\bar{h}_{nm}(\tau)$ is a substitution of $\bar{h}$ in Eq. (26) for impulse response $\bar{h}_{nm}$ of path $nm(m = 1, 2, \ldots, M; n = 1, 2, \ldots, N)$. In the equation, k'' is an integer that represents discrete time, and the range in which k'' makes a substantial contribution is equivalent to the spread of delay beginning in the vicinity of 0.

Another channel representation that can be employed with respect to broadband signals is a frequency-domain representation. In this case, it suffices to represent the channel response characteristics of Eqs. (3)–(7) that represent narrow-band signals as a function of frequency. They can be expressed as follows.

$$A(f) = [a_{nm}(f)] \tag{34}$$

$$\begin{aligned} a_{nm}(f) &= \int_{-\infty}^{\infty} h_{nm}(\tau) \exp(-j2\pi f\tau) d\tau \\ &\approx \int_{-\infty}^{\infty} \bar{h}_{e,nm}(\tau) \exp(-j2\pi f\tau) d\tau \end{aligned} \tag{35}$$

As a result, the correlation matrices, eigenvalues, and eigenvectors can all be represented as a function of frequency. The channel matrix A can then be processed by singular-value decomposition as follows.

$$\begin{aligned} A(f) &= E_r(f) D(f) E_t^H(f) \\ &= \sum_{i=1}^{M_0} \sqrt{\lambda_i(f)}\, \boldsymbol{e}_{r,i}(f) \boldsymbol{e}_{t,i}^H(f) \end{aligned} \tag{36}$$

Although the eigenvalues change continuously in their respective bands, in some cases, two eigenvalues, such as the first and second eigenvalues, change in such a way that they intersect. Even in that case, continuity can be maintained within the band due to the fact that the maximum eigenvalue $\lambda_{\max}(f)$ is always maximum. However, eigenvectors belonging to the maximum eigenvalue are exchanged at the point where two eigenvalues become equal and intersect, thus resulting in a loss of continuity. Such a situation poses a risk of control instability, as will be discussed in Sect. 5.

In a system such as that of orthogonal frequency-domain multiplexing (OFDM), where every signal in the time series is expanded as a narrow-band signal in the frequency domain, the characteristic of each subchannel can be defined as a carrier wave frequency corresponding to the signal. Therefore, the expression in Eq. (36) can be directly applied to the analysis of the MIMO-OFDM information transmission method and the relevant transmission characteristics [6], [7].

To summarize the discussion above, Fig. 9 shows an example of a broadband MIMO transmission path (a) in terms of the time domain (b) based on Eq. (33) and the frequency domain (c) based on Eq. (34).

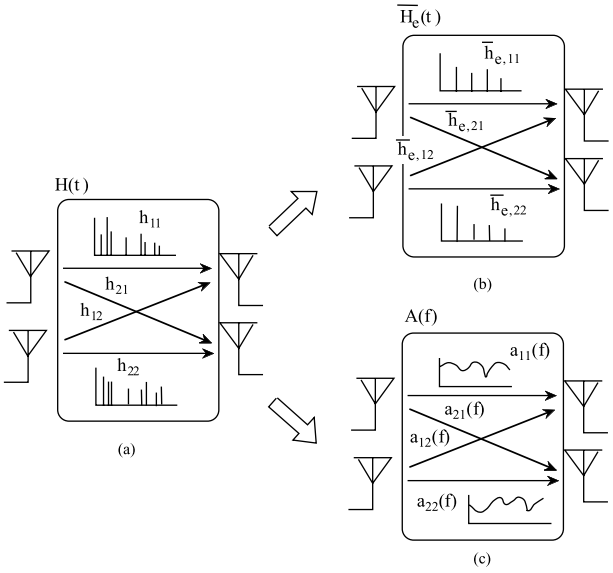

Fig. 9 Modeling of wideband MIMO propagation channel.

4. Statistical Representation of the MIMO Channel

4.1 Independent Identically Distributed Channels (Model 1)

In mobile communications, the movement of terminals causes multipath problems that manifest as temporal fluctuations. By contrast, in wireless LAN, where terminals are stationary desktops, the characteristics manifest as spatial changes. In either case, it is critical to have a statistical understanding of the multipath characteristics. In this section, the Model 1 environment depicted in Fig. 1 is considered. This case represents an environment in which there are a large number of paths with sufficiently large angular spread at both transmitting and receiving stations. In Fig. 2, if the distance of separation between antennas is half the wavelength or greater, the correlation coefficient will be 0.5 or less, and thus the impact of correlation is negligible. In this environment, the amplitudes of all paths a_{nm} in Fig. 6(a) have the same Rayleigh distribution, and their fluctuations can be treated as independent quantities. Such channels are referred to as independent identically distributed (i.i.d.) channels.

The statistical characteristics of the i.i.d. channels, that is, the probability distribution of eigenvalues of the correlation matrix, are examined as follows. In the multipath environment, power fluctuations in the Rayleigh fading environment take the form of an exponential distribution. In the 1-to-N maximum ratio combining diversity, the distribution becomes a gamma distribution. MIMO represents a dimensional expansion of that distribution to M-to-N, for which the individual matrix elements and eigenvalues take the form of a Wishart distribution [19]–[22]. Figure 10 shows the cumulative distribution of eight eigenvalues of the correlation matrix AA^H where $M = N = 8$. The distribution

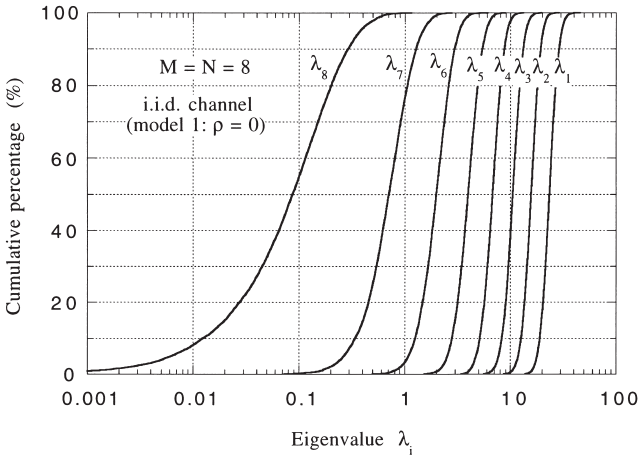

Fig. 10 CDF of each eigenvalue for $M = N = 8$ in i.i.d. Rayleigh fading channel.

shown in the figure was obtained by computer simulations. The theory behind the determination of this distribution is well established in the field of numerical statistics, and an equation for obtaining the cross-coupled probability distribution of all eigenvalues is available (not quoted here because the equation is of little practical value for computation purposes; the equation is indicated in Ref. [27] as quoted from Ref. [21]).

In the maximal ratio combining transmission (beamforming transmission) of MIMO, the value of the largest eigenvalue, $\lambda_{\max}$, provides an index for the evaluation of performance. For the probability distribution of maximum eigenvalues, the following equations are obtained by integrating other eigenvalues from the cross-coupled probability distribution of all eigenvalues as probability variables [22]:

$$f(\lambda_{\max}) = \frac{1}{P}\sum_{p=1}^{P}\varphi_p(\lambda_{\max})^2\lambda_{\max}^{Q-P}e^{-\lambda_{\max}} \tag{37a}$$

$$\varphi_{k+1}(\lambda) = \sqrt{\frac{k!}{(k+Q-P)!}}L_k^{Q-P}(\lambda) \tag{37b}$$

$$(k = 0,\ 1,\ \ldots,\ P-1)$$

$$L_k^{Q-P}(x) = \frac{1}{k!}e^x x^{Q-P}\frac{d^k}{dx^k}(e^{-x}x^{Q-P+k}) \tag{37c}$$

$$P(\equiv M_0) \equiv \min(M,N),\ Q \equiv \max(M,N). \tag{37d}$$

The actual computation of the above equations will not be easy when the value of M, N, or Q is large. To circumvent this problem, research on approximation techniques is being pursued to determine a distribution by linking the $M \times N$-configuration MIMO to a $1 \times MN$-configuration SIMO (single-input multiple-output) space diversity [27]. With i.i.d. channels, determining the probability distribution of the largest eigenvalues of the $M \times N$-configuration MIMO by computer simulation (for example, λ_1 in Fig. 10), and comparing the results with the SN ratio distribution (gamma distribution) for the maximum ratio combining for 1-to-MN space diversity yields a high degree of agreement with regard to distribution profiles [27]. This means that the probability distribution of the first eigenvalues of the $M \times N$-configuration MIMO can also be approximated by a gamma distribution. To complete this distribution as an algorithm, it is necessary to obtain an equation that gives the average of the maximum eigenvalues. To this end, an approximation formula has been proposed [27]. The following is an algorithm (gamma distribution, where f denotes a probability density function, and F denotes a cumulative distribution function) that gives the distribution of the maximum eigenvalues obtained in this manner:

$$f(\lambda_{\max}) = \frac{1}{(MN-1)!}\frac{\lambda_{\max}^{MN-1}}{\Gamma_0^{MN}}\cdot\exp\left(-\frac{\lambda_{\max}}{\Gamma_0}\right) \tag{38a}$$

$$F(\lambda_{\max}) = 1 - \exp\left(-\frac{\lambda_{\max}}{\Gamma_0}\right)\cdot\sum_{j=1}^{MN}\frac{(\lambda_{\max}/\Gamma_0)^{j-1}}{(j-1)!}, \tag{38b}$$

where Γ_0 is the average of the maximum eigenvalues normalized by MN. It can effectively be approximated by the following equation (for further details, see Ref. [27]):

$$\Gamma_0 = \langle\lambda_{\max}\rangle/MN \begin{cases} \approx \left(\dfrac{M+N}{MN+1}\right)^{2/3} \\ \qquad \text{for } NM \le 250 & \text{(39a)} \\ \approx \left(\sqrt{M}+\sqrt{N}\right)^2/MN \\ \qquad \text{for } NM > 250. & \text{(39b)} \end{cases}$$

Comparing with values obtained by computer simulation, it has been found that the estimation using Eq. (38) is sufficiently accurate for practical purposes [27]. It should be noted that Eq. (39b) is derived as an asymptotic formula (or an equation that provides an upper bound on the averages) when both N and M are sufficiently large [13].

4.2 Distribution of Maximum Eigenvalues Considering Spatial Correlation

The Model 2 environment shown in Fig. 1 requires an analysis that takes into account spatial correlation on the base station side where the angular spread in the direction of the path is relatively small. Figure 11 shows the average eigenvalues, obtained by simulation, for the $M = N$-configuration MIMO, for which spatial correlation can be ignored (Model 1: i.i.d. channel) and for the case where a correlation exists only on one side (Model 2) [23]. An array of antennas placed at equal intervals on a straight line is employed, and the correlation between elements is set so as to yield the values calculated according to Eq. (2) in all combinations. In the figure, the value $\rho(\equiv|\rho_a(d)|)$ of the correlation is defined as a correlation coefficient in terms of the nearest antenna element distance d for the side that takes the correlation into account. Figure 11(b) shows the case where this value is 0.9. The figure indicates that, in comparison to the case with no correlation, the largest eigenvalue is more dominant when

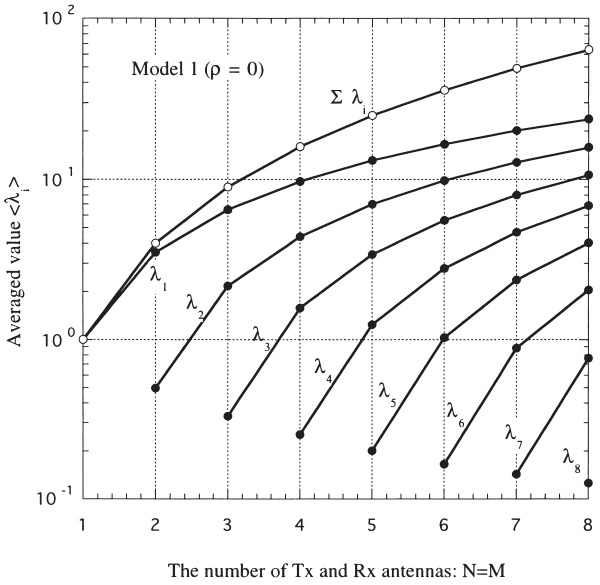

(a) Model 1 (i.i.d. channel; ρ = 0)

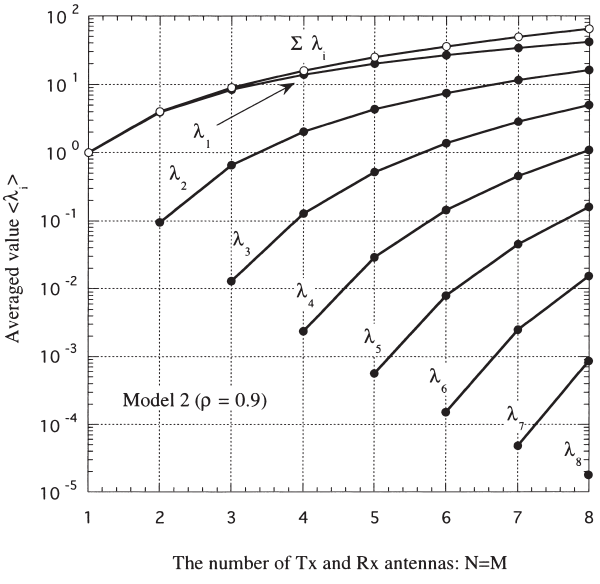

(b) Model 2 (ρ= 0.9)

Fig. 11 Averaged value of each eigenvalue depending on spatial correlation.

there is correlation, and the second and subsequent eigenvalues are relatively small. In the figure, the line connected by ∘ represents the sum ($= N^2$) of all eigenvalues.

Analyses of transmission characteristics taking correlation into account have been attempted [16], [17]. However, to date, no mathematical models have been established that provide a probability distribution of eigenvalues with a simple form. For consistency with the approximation model described in Sect. 4.1, the diversity approximation model given in reference [23] is considered hereafter.

Defining a new vector $\boldsymbol{b}$ as

$$\boldsymbol{b} \equiv \left[\boldsymbol{a}_1^T\ \boldsymbol{a}_2^T\ \ldots\ \boldsymbol{a}_m^T\ \ldots\ \boldsymbol{a}_M^T\right]^T \tag{40}$$

to represent all paths in one vector using the column vector $\boldsymbol{a}$ in the channel response matrix A of Eq. (3), the correlation matrix among paths is as follows:

$$\tilde{R}_{aa} = \langle \boldsymbol{b}\boldsymbol{b}^H \rangle \tag{41a}$$

$$\approx \begin{bmatrix} \langle \boldsymbol{a}_1\boldsymbol{a}_1^H\rangle & \mathbf{0} & \cdots & \mathbf{0} \\ \mathbf{0} & \langle \boldsymbol{a}_2\boldsymbol{a}_2^H\rangle & \cdots & \mathbf{0} \\ \vdots & \vdots & \ddots & \vdots \\ \mathbf{0} & \mathbf{0} & \cdots & \langle \boldsymbol{a}_M\boldsymbol{a}_M^H\rangle \end{bmatrix} \quad \text{(model 2)} \tag{41b}$$

$$\approx I_{NM} \quad \text{(model 1)}. \tag{41c}$$

where $\langle\ \rangle$ is the average over a sufficiently long time compared with the fading fluctuation cycles (or a sufficiently long distance with respect to space changes when compared with the cycles of fluctuation), and I_{NM} denotes the unit matrix of $NM \times NM$.

This matrix contains NM eigenvalues, which can be sorted in descending order as $[\tilde{\lambda}_1 \sim \tilde{\lambda}_{NM}]$. In Model 1 (Eq. (41c)), all eigenvalues are equal to 1. In Model 2 (Eq. (41b)), if the MT side in Fig. 1(b) is assumed to have M elements and the BS side has N elements, N sets of M equal values are obtained.

In this case, the probability distribution of the maximum eigenvalues $\lambda_{\max}$ in AA^H can be estimated by linking the distribution to Eq. (25) to give the probability distribution of the SNR in a correlated 1-to-MN space diversity, as given by [23]

$$f(\lambda_{\max}) = \frac{1}{\prod_{j=1}^{MN}\Gamma_j} \sum_{j=1}^{MN} \frac{\exp(-\lambda_{\max})/\Gamma_j)}{\prod_{\substack{k\neq j\\ k=1}}^{MN}\left(\frac{1}{\Gamma_k}-\frac{1}{\Gamma_j}\right)} \tag{42a}$$

$$F(\lambda_{\max}) = 1 - \sum_{j=1}^{MN} \frac{\Gamma_j^{MN-1}\exp(-\lambda_{\max}/\Gamma_j)}{\prod_{\substack{k\neq j\\ k=1}}^{MN}(\Gamma_j-\Gamma_k)} \tag{42b}$$

$$\Gamma_j = (\tilde{\lambda}_j + \varepsilon_j)G(M,N;\rho)/MN \tag{42c}$$

$$\tilde{\lambda}_j \gg \varepsilon_j, \tag{42d}$$

where ε_j denotes a very small quantity assigned to avoid the possibility of Eqs. (42) becoming uncomputable if eigenvalues are identical. Similarly, $G(M,N;\rho)$ denotes the average of the maximum eigenvalues $\lambda_{\max}$. In the case of Model 1, the following approximation formula exists for $G(M,N;\rho)$ [23]:

$$G(M,N;\rho) = MN\left\{\alpha + \left(\frac{M+N}{MN+1}\right)^{2/3}(1-\alpha)\right\} \tag{43a}$$

$$\alpha = \left(\frac{\sum_{j=1}^{N}\tilde{\lambda}_j - N}{MN-1}\right)^{3/\sqrt{M}}. \tag{43b}$$

Due to the fact that the above equations are based on

Eq. (39a) as the model, $MN < 250$ is the approximate criterion for applying the above equations.

This discussion has only considered estimation methods based on the approximation of the largest eigenvalues for which a correlation exists. The establishment of a theoretical or approximation model for the determination of the probability distribution of all eigenvalues remains an important topic.

4.3 Channel Capacity

According to Shannon's information theory, if a transmission channel has an SNR of γ, the transmission channel capacity C per second per Hz is given by

$$C = \log_2(1 + \gamma) \qquad \text{[bits/s/Hz]}. \tag{44}$$

In MIMO, the following two cases, illustrated in Fig. 5, yield different channel capacities.
Case 1: Only the receiver has information on a MIMO channel response matrix
Case 2: Both the transmitter and receiver share information on the MIMO channel (based on prior measurements and other factors)

In Case 1, the transmission capacity is given by

$$C_1 = \sum_{i=1}^{M_0} \log_2\left(1 + \frac{\lambda_i \gamma_0}{M}\right), \tag{45}$$

where γ_0 denotes the SNR when all power from the transmitter is emitted from a single antenna and is received on a single antenna after traversing paths with a path gain of 1. This means that the maximum capacity is achieved when the transmitter does not know the conditions under which transmission is performed and the power is distributed uniformly to all transmitting antennas (i.e., by avoiding a worst-case scenario where null points arise in a specific direction).

In Case 2, the transmission capacity is given by

$$C_2 = \sum_{i=1}^{M_0} \log_2(1 + \lambda_i \gamma_i) \tag{46a}$$

$$\sum_{i=1}^{M_0} \gamma_i = \gamma_0. \tag{46b}$$

In this case, a power proportional to γ_i is allocated to each eigenpath, and the optimum allocation is based on the Water Filling (WF) theorem (for a specific allocation method based on the WF theorem, see Ref. [28]). The transmission capacity that is optimally allocated according to the WF theorem is referred to as C_{WF}.

In Case 2, the method in which all power is allocated only to the largest eigenpath (primary path) having the maximum eigenvalue is an MRC method with controlled transmission/reception weights. In this case, the transmission capacity is given by

$$C_{\mathrm{MRC}} = \log_2(1 + \lambda_1 \gamma_0). \tag{47}$$

The transmission path capacity of the MIMO channel in the Rayleigh fading environment can be calculated as follows, using the cross-coupled probability density function of eigenvalues $f(\lambda_1, \lambda_2, \ldots, \lambda_{M_0})$:

$$\langle C \rangle = \iint \cdots \int_0^\infty C(\lambda_1,\ \lambda_2,\ \ldots,\ \lambda_{M_0}) \cdot f(\lambda_1,\ \lambda_2,\ \ldots\ \lambda_{M_0}) d\lambda_1\, d\lambda_2\, \ldots\, d\lambda_{M_0}. \tag{48}$$

However, including no-correlation cases, there is no simple algorithm for calculating the cross-coupled probability density function f of eigenvalues. Therefore, the following approximation formula using the average of the eigenvalues is often used:

$$\langle C \rangle = C\left\{\langle \lambda_1 \rangle,\ \langle \lambda_2 \rangle,\ \ldots,\ \langle \lambda_{M_0} \rangle\right\}. \tag{49}$$

It has been determined, for MRC transmission calculated solely on maximum eigenvalues (i.e., calculated according to Eq. (47)), that the difference between the calculated values based on the probability distribution of eigenvalues and those calculated according to average values can be ignored [27]. Therefore, it is expected that Eq. (49) will also yield a high degree of accuracy.

Figure 12 shows the calculated averages of C_1, C_{WF}, and C_{MRC} for iid channels based on the algorithm (Eqs. (45)–(47)) for channel capacity. To permit a comparison of the three channel capacities on an equal basis, it is assumed that the total transmitting power is constant, and that the channel bandwidth (or the bandwidth of transmitted signals) is fixed. In the figure, γ_0 is used as a parameter, which is equivalent to the SNR. The figure shows three cases: $\gamma_0 = 0.1$ (extremely poor SNR), $\gamma_0 = 1$, and $\gamma_0 = 10$

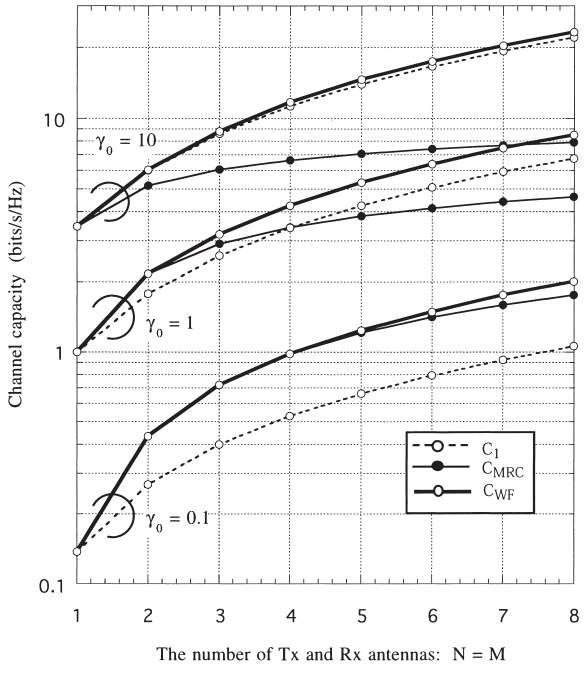

Fig. 12 Comparison of channel capacity for three transmission schemes.

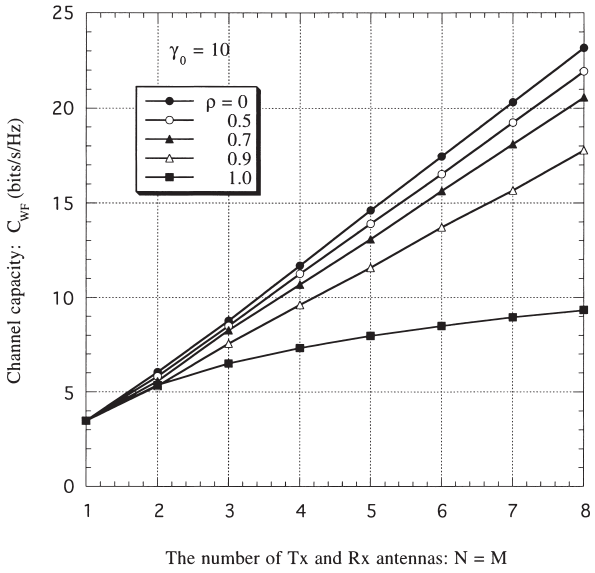

Fig. 13 Effect of correlation on channel capacity C_{WF} in higher SNR case.

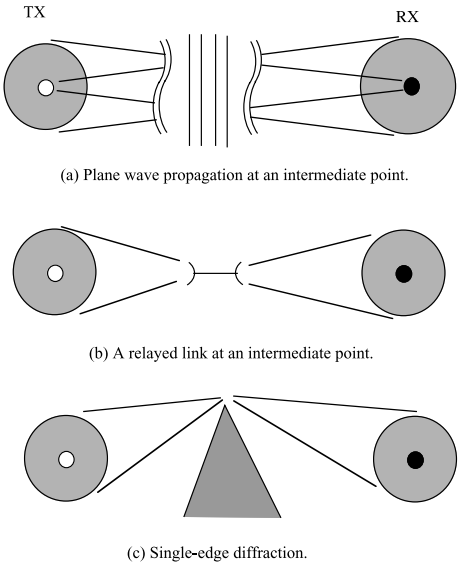

Fig. 14 Propagation environments consisting of only one eigenpath.

(high SNR). It can be seen from the figure that, (i) where the SNR of the transmission path is low, near-limit performance can be obtained for MRC by allocating all power to the maximum eigenpath (the primary path), and (ii) where the SNR is high, a higher channel capacity can be obtained by allocating some power to other eigenpaths (secondary paths). It can also be appreciated that as the SNR increases, the difference between Case 1 (C_1) and Case 2 (C_{WF}) vanishes. Figure 13 shows the channel capacity C_{WF} including correlation-rich cases, for $\gamma_0 = 10$, which is a high SNR environment, by using the correlation coefficient as a parameter. The figure indicates that when optimal transmission is to be conducted, the impact of correlation results in a decline in channel capacity. The analysis of channel capacities indicates that it is important to understand the eigenvalue distribution interms of a radio wave propagation characteristic. The same is true of the evaluation of bit error rates (BERs). Therefore, MIMO propagation channel modeling, in essence, is the investigation of the characteristics of eigenvalues of channel response matrices.

5. Impact of Radio Wave Propagation Environment on MIMO Transmission Characteristics

5.1 Case of Eigenpaths Reducing to One Path

Even in a multipath-rich environment where the area around the transmitting station and the area around the receiving station are surrounded by local scatterers, and where the angular spreading in the direction of the path is large, the second and subsequent eigenvalues reduce to zero, and only the first eigenvalue predominates in some cases as shown in Fig. 14. This means that in the modeling of MIMO channels, in addition to both the propagation environment around the transmitting and receiving stations, the intervening propagation structure exerts a significant influence on the MIMO transmission characteristics.

Figure 14(a) illustrates the case where the range of angles at which the receiving antenna has a clear view of the scattering area at the transmission point and the range of angles at which the transmitting antenna has a clear view of the scattering area at the reception point are both sufficiently smaller than the antenna beam width. Therefore, that in this environment, plane waves reach the destination area (the case in Fig. 4(b) also corresponds to this scenario). The same is true of the situation in Fig. 14(b) where signals are relayed by means of a single antenna. This case has previously been treated as a keyhole problem [15]. Another example, as shown in Fig. 14(c), involves the arrival of diffracted waves only from the edge of a single scatterer (building).

In all of these cases, the SVD representation of the channel response matrix A takes the form of

$$A \approx \sqrt{\lambda_1}\, \boldsymbol{e}_{r,1} \boldsymbol{e}_{t,1}^{H}, \tag{50}$$

where the eigenvalues for the correlation matrix AA^H (and A^HA) collapse into one eigenvalue (i.e., the correlation matrix becomes a matrix of Rank 1). In this case, as may be clear from Fig. 14, because the multipath environment for the area around the terminal is maintained, a space diversity effect (improvement in combined gains and suppression of fluctuations) can be expected. However, from a standpoint of multistream transmission, the degree of freedom is lost. This situation can be understood as being a cascade connection of a multiple-input single-output (MISO) channel to a single-input multiple output (SIMO) channel.

From a high-efficiency information transmission standpoint, an optimal environment is one in which multiple independent paths (eigenpaths), typically the indoor multipath environment, can exist. Therefore, wireless LAN represents an environment in which MIMO can operate to its full po-

tential.

5.2 Inherent Instability of MIMO Weight Control

In a situation where the propagation environment changes as a function of time, there is an inherent instability problem in MIMO control when the weights of transmission and reception are controlled based on an adaptive algorithm, as illustrated in the following example.

Consider control involving MRC. Let $\lambda_i(t)(i = 1, 2, \dots M_0)$ be the eigenvalues of a correlation matrix, and assign numbers i to the eigenvalues that vary continuously (unlike the situation discussed in Sect. 2, the eigenvalues are not in descending order). In this case, the MRC method is an algorithm with a weight equal to an eigenvector that always produces the maximum eigenvalue, that is,

$$\lambda_{\max}(t) = \max\{\lambda_1(t),\ \lambda_2(t),\ \dots,\ \lambda_{M_0}(t)\} \tag{51}$$

Because the quantity λ_i changes continuously as a function of time, $\lambda_{\max}$ also changes continuously. However, the weight that implements the quantity loses continuity each time the selection changes in Eq. (51). In addition, in situations where the transmitting and receiving stations both measure transmission characteristics (as in the TDD method, for example) and control weights are determined independently, as the difference between the maximum eigenvalue and the second eigenvalue becomes smaller, a mismatch between transmitter and receiver weights is likely to occer. Further more when the first and second eigenvalues are equal by coincidence, the resulting eigenvector instability and transmission/reception mismatch increases the possibility of a significant decline in the reception signal strength [29]. Therefore, for practical control purposes, it is necessary to avoid this risk.

Although instability and discontinuity have been discussed as problems of control in the time domain, similar problems can occur between subchannels in the frequency domain, such as the control of OFDM subchannels. The issue of discontinuity as a result of null-forming by transmission/reception using an adaptive array is addressed in Ref. [18]. This is a difficult problem that cannot be ignored in systems in which adaptive control is performed by both the transmitter and the eceiver.

6. Research Topics Relevant to MIMO Radio Wave Propagation

Research in information theory, such as that on channel capacity (Eqs. (45)–(47)) or the corresponding space-time coding, will be substantially facilitated at the conceptual level if the propagation models can be organized as depicted in Fig. 6(b). Radio wave propagation, on the other hand, is subject to an extremely complex set of environmental factors. Consequently, before a radio wave propagation model involving MIMO channels can be established, many issues must be studied. Until now, knowledge of the radio wave environment of the areas surrounding either the mobile station or base station has provided a sufficient foundation for the development of a SIMO radio wave propagation mode. In MIMO, on the other hand, the propagation structure of the intervening paths also affects the distribution of correlation matrix eigenvalues, necessitating research by novel approaches.

The research relevant to radio wave propagation that remains to be undertaken includes the following topics.

(1) Analysis of how eigenvalues are distributed in a specific propagation environment (propagation measurement and propagation channel modeling).
(2) Analysis of how MIMO beam forming should be configured in concrete terms such as antenna configuration, and dual polarization, etc.
(3) Development of methods for antenna weight control based on these topics (adaptive algorithm; in particular, a robust control algorithm dealing with the problem of discontinuity inherent in weight control).
(4) Development of methods for a more efficient information transmission scheme (space-time coded transmission, power distribution by water-filling).
(5) Configuration and characteristic evaluation with application to wideband systems such as CDMA and OFDM.
(6) Analysis of how MIMO channel characteristics can be determined in real time (measurement and estimation of channel characteristics).

In particular, for a propagation environment subject to extensive temporal fluctuations, solving problems (3) and (6) can be a challenging task, and many issues must be overcome. Furthermore, MIMO information transmission (5) over a wide-band channel, a topic that was limited to the representation of channels in this paper, involves an extremely complex treatment at both the mathematical and configurational levels, and requires study from the fundamentals.

MIMO is literally a multiple-input, multiple-output transmission method, and it is not necessary for array antennas to be employed. As stated in Item (2), any mode, for example, antenna/polarized wave/frequency slots, that composes a diversity branch in the ordinary sense can be employed. From a radio wave propagation standpoint, it may be interesting to incorporate orthogonal polarized waves into an $M \times N$ array to implement $2M \times 2N$ space-polarization-combined MIMO transmission. To fully exploit the capabilities of MIMO, it is necessary to keep track of the behavior of the channel response matrix in real time (6). Thus, there remain many topics of research at the system level, such as whether the same frequency must be used at the transmitting and receiving ends (i.e., TDD or FDD), and how to incorporate pilot signals for channel monitoring.

7. Conclusions

MIMO has the potential to surpass the capabilities of combined transmission and reception adaptive arrays. The out-

standing potential performance of MIMO can be summarized by the performance = "gains due to use of an array antenna for the transmitting station" × "gains due to the use of an array antenna for the receiving station" × "the number of multiple streams." MIMO can utilize not only the largest path based on the largest eigenvalue in the equivalent circuit, but also secondary paths based on the second and lower eigenvalues, although the latter effect depends on the complex interplay of both the propagation environment including Tx and Rx site environments and intervening propagation structure and the number of antennas deployed. In this paper, typical examples operating in a Rayleigh fading environment were presented. The question as to whether the benefits offered by MIMO (Fig. 12) are significant or relatively trivial must be judged, taking the difficulty of implementation into account.

Starting from fundamental examples such as the narrow band, i.i.d. Rayleigh fading, time invariance, and the absence of interference waves, we have touched upon topics at the forefront of research, such as wideband representations and interpath correlations. Research efforts based on radio wave propagation must therefore begin from the topics covered in this paper, and a number of issues await exploration. It is hoped that this paper will provide some valuable suggestions for future research and development efforts in MIMO technology.

Finally, the author thanks Dr. T. Taniguchi of the University of Electro-Communications and Dr. Y. Zhang of Villanova University (USA) for valuable discussion. Gratitude is also extended to Dr. K. Sakaguchi of the Tokyo Institute of Technology for providing valuable information on the Wishert distribution. The assistance of Mr. M. Tsuruta and Miss J. Fu, graduate students of the Karasawa Laboratories of the University of Electro-Communications, in the preparation of some of the drawings is also appreciated.

References

[1] J. Salz, "Digital transmission over cross-coupled linear channels," AT&T Tech. J., vol.64, no.6, pp.1147–1159, July–Aug. 1985.

[2] J.H. Winters, "On the capacity of radio communications systems with diversity in Rayleigh fading environments," IEEE J. Sel. Areas Commun., vol.5, no.5, pp.871–878, 1987.

[3] J. Yang and S. Roy, "On joint transmitter and receiver optimization for multiple-input multiple-output (MIMO) transmission systems," IEEE Trans. Commun., vol.42, no.12, pp.3221–3231, 1994.

[4] G.J. Foschini, "Layered space-time architecture for wireless communication in a fading environment when using multi-element antennas," Bell Labs. Tech. J., vol.1, no.2, pp.41–59, 1996.

[5] R.D. Murch and K.B. Letaief, "Antenna systems for broadband wireless access," IEEE Commun. Mag., vol.40, no.4, pp.70–83, April 2002.

[6] K. Wong, R.S. Cheng, K.B. Letaief, and R.D. Murch, "Adaptive antennas at the mobile and base stations in an OFDM/TDMA systems," IEEE Trans., Veh. Technol., vol.49, no.1, pp.195–206, 2001.

[7] Y. Karasawa, T. Taniguch, and Y. Zhang, "On multiple-input multiple-output (MIMO) maxmal ratio combining (MRC) and optimal data transmission for OFDM," IEICE Technical Report A · P2001-196, 2002.

[8] K. Miyashita, T. Nishimura, T. Ohgane, Y. Ogawa, Y. Takatori, and K. Cho, "High data-rate transmission with eigenbeam-space division multiplexing (E-SDM) in a MIMO channel," Proc. IEEE VTC 2002-Fall, vol.3, pp.1302–1306, Sept. 2002.

[9] S.M. Alamouti, "A simple transmit technique for wireless communications," IEEE J. Sel. Areas Commun., vol.16, no.8, pp.1451–1458, 1998.

[10] V. Tarokh, N. Seshadri, and A.R. Calderbank, "Space-time codes for high data rate wireless communication: Performance critrion and code construction," IEEE Trans. Inf. Theory, vol.44, no.2, pp.744–765, 1998.

[11] G.G. Raleigh and J.M. Cioffi, "Spatio-temporal coding for wireless communication," IEEE Trans. Commun., vol.46, no.3, pp.357–366, 1998.

[12] R.W. Heath, Jr. and A.J. Paulraj, "Capacity maximizing linear space-time codes," IEICE Trans. Electron., vol.E85-C, no.3, pp.428–435, March 2002.

[13] J.B. Andersen, "Array gain and capacity for known random channels with multiple element arrays at both ends," IEEE J. Sel. Areas Commun., vol.18, no.11, pp.2172–2178, 2000.

[14] J.F. Kepler, T.P. Krauss, and S. Mukthavaram, "Delay spread measurements on a wideband MIMO channels at 3.7 GHz," 2002 IEEE VTC-Fall, Vancouver, Sept. 2002.

[15] D. Chizhik, G.J. Foschini, M.J. Gans, and R.A. Valenzuela, "Keyholes, correlations, and capacities of multielement transmit and recive antennas," IEEE Trans. Wireless Commun., vol.1, no.2, pp.361–368, 2002.

[16] D.S. Shiu, G.J. Foschini, M.J. Gans, and J.M. Kahn, "Fading correlation and its effect on the capacity of multielement antenna systems," IEEE Trans. Commun., vol.48, no.3, pp.502–513, 2000.

[17] S.Y. Loyoka, "Channel capacity of MIMO architecture using the exponential correlation matrix," IEEE Trans. Commun. Lett., vol.5, no.9, pp.369–371, 2001.

[18] Y. Karasawa, "On data transmission capability of MIMO channel from a wave propagation viewpoint," IEICE Technical Report A · P2002-101, 2002.

[19] A.T. James, "Distributions of matrix variates and latent roots derived from normal samples," Ann. Math. Statist., vol.35, pp.475–501, 1964.

[20] A.T. James, "The distributions of the latent roots of the covarience matrix," Ann. Math. Statist., vol.31, pp.151–158, 1960.

[21] A. Edelman, "Eigenvalues and condition numbers of random matrices," SIAM J. Matrix Anal. Appl., vol.9, no.4, pp.543–560, Oct. 1998.

[22] S.S. Wilks, Mathmatical Statistics, Wiley, New York, 1962.

[23] J. Fu, T. Taniguchi, and Y. Karasawa, "The largest eigen value characterisstics for MIMO channel with spatial correlation," IEICE Trans. Commun. (Japanese Edition), vol.J86-B, no.9, pp.1971–1980, Sept. 2003.

[24] Y. Karasawa, Radiowave Prppagation Fundamental in Digital Mobile Communications, Corona Pub., 2003.

[25] W.C.Y. Lee, Mobile communication engineering, McGraw-Hill, 1982.

[26] Y. Karasawa and T. Inoue, "Real-time simulation scheme of mobile radio propagation channel based on a statistical model," J. IEICE, vol.83, no.11, pp.884–888, 2000.

[27] J. Fu, T. Taniguchi, and Y. Karasawa, "Simplified estimation method for MRC transmission characteristics in Rayleigh iid MIMO channel," IEICE Trans. Commun. (Japanese Edition), vol.J86-B, no.9, pp.1963–1970, Sept. 2003.

[28] J.G. Proakis, Digital communications, 3rd ed., McGraw-Hill, New York, 1995.

[29] R. Takemoto, T. Taniguchi, and Y. Karasawa, "Eigenvector mismatch problem and its countermeasure for MIMO MRC transmission,—In the case of inter-vehicle communications at 60 GHz," IEICE Trans. Commun. (Japanese Edition), vol.J87-B, no.9, pp.1477–1485, Sept. 2004.

Yoshio Karasawa received B.E. degree from Yamanashi University in 1973 and M.S. and Dr. Eng. Degrees from Kyoto University in 1977 and 1992, respectively. He joined KDD R&D Labs. in 1977. From July 1993 to July 1997, he was a Department Head of ATR Optical and Radio Communications Res. Labs. and ATR Adaptive Communications Res. Labs., both in Kyoto. Currently, he is a professor of the University of Electro-Communications, Tokyo. Since 1977, he has been engaged in studies on wave propagation and radio communication antennas, particularly on theoretical analysis and measurements for wave-propagation phenomena, such as multipath fading in mobile radio systems, tropospheric and ionospheric scintillation, and rain attenuation. His recent interests are in frontier regions bridging "wave propagation" and "digital transmission characteristics" in wideband mobile radio systems such as MIMO. Dr. Karasawa received the Young Engineers Award from the IECE of Japan in 1983 and the Meritorious Award on Radio from the Association of Radio Industries and Businesses (ARIB, Japan) in 1998. He is a member of the IEEE, SICE and URSI.